A Mechanobiologically Equilibrated Kinematic Growth Model for Soft Tissues

A. Bezmalinovic[1], C. García-Herrera[1], D. Celentano[2] and M. Latorre[3]

[1]Department of Mechanical Engineering,
Universidad de Santiago de Chile, Chile
[2]Department of Mechanical and Metallurgical Engineering,
Pontificia Universidad Católica de Chile, Santiago, Chile
[3]Center for Research and Innovation in Bioengineering,
Universitat Politècnica de València, Spain

Abstract

The concept of mechanobiological equilibrium (MBE) is incorporated into the finite kinematic growth (KG) model for growth and remodelling (G&R), in order to propose an alternative, rate-independent formulation (MBE-KG). The method proposed yields non-transient solutions to G&R problems and quasi-equilibrated evolutions when imposed perturbations are slow relative to the adaptive process. We perform a finite element implementation of the method and show its performance on some illustrative problems involving the simulation of aneurysms on a single-layered artery model.

Keywords: growth and remodelling, kinematic growth, mechanobiological equilibrium, finite element method, artery, aneurysm

1 Introduction

One of the main characteristics of biological materials is their ability to grow (change mass) and remodel (change structure) in response to mainly mechanical and biochemical stimuli. Cells strive to attain, preserve, or regain a homeostatic [1] mechanical state and ultimately, under stable physiological conditions, attain a state of mechanobiological equilibrium [2]. Homeostasis and mechanobiological equilibrium are analogous concepts, mathematically represented by a unit value of a stimulus function [3].

In this paper, we present a rate-independent finite kinematic growth (KG) model for growth and remodelling (G&R) of soft tissues, by imposing mechanobiological equilibrium on its classical, rate-dependent counterpart first proposed in [4]. To our knowledge, this approach has only been applied to the constrained mixtures (CM) G&R model [5, 6], in which constituent-specific hyperelastic descriptors and rates of production and removal are considered [7].

2 A mechanobiologically-equilibrated finite kinematic growth model

The mass balance for open systems is governed by the evolution equation, $\dot{\rho} + \rho \operatorname{div}(\mathbf{v}) = \bar{m}$, where ρ is the spatial mass density, $\dot{\rho}$ its material time derivative, $\operatorname{div}(\mathbf{v}) = \dot{J}/J$ is the velocity, with $J = \det(\mathbf{F})$ the Jacobian determinant of the deformation gradient, $\mathbf{F} \in \mathrm{GL}(3)$, and $\bar{m} = m - r \neq 0$ is the net rate of mass density, defined in terms of true rates of mass density production ($m > 0$) and removal ($r > 0$), that in turn defines a stimulus function, $\Upsilon = m/r > 0$ [3]. The stimulus function represents the enhancement ($\Upsilon > 1$), reduction ($\Upsilon < 1$) or balance ($\Upsilon = 1$) of mass production with respect to removal.

A kinematic growth (KG) model postulates a multiplicative decomposition of the deformation gradient [4]:

$$\mathbf{F} = \mathbf{F}_{\mathrm{e}} \, \mathbf{F}_{\mathrm{g}}, \tag{1}$$

into an elastic part $\mathbf{F}_{\mathrm{e}}$, that generates mechanical stresses, and an inelastic (growth) part $\mathbf{F}_{\mathrm{g}}$, that represents a local addition or subtraction of mass. Usually, the growth component of the deformation gradient is characterized via a single scalar variable (growth multiplier, ϑ), such that $\det(\mathbf{F}_{\mathrm{g}}) = \vartheta$. For instance, in isotropic volumetric growth, $\mathbf{F}_{\mathrm{g}} = \vartheta^{1/3} \mathbf{1}$, where $\mathbf{1}$ is the second-order unit tensor.

Since soft tissues tend to preserve their overall density, $\dot{\rho} = 0$. Further assuming an incompressible elastic behavior (i.e. $\det(\mathbf{F}_{\mathrm{e}}) = 1$), the mass-balance equation takes the form [3], $\dot{\vartheta}/\vartheta = k\,(\Upsilon - 1)$, where $k = r/\rho$ is a rate parameter.

Let $\mathbf{C} = \mathbf{F}^{\mathrm{T}} \mathbf{F}$, be the right Cauchy-Green strain. Then, as a consequence of the multiplicative decomposition for the deformation gradient (Equation 1), the elastic

Cauchy-Green strain is, $\mathbf{C}_e = \mathbf{F}_g^{-T} \mathbf{C} \, \mathbf{F}_g^{-1} = \mathbf{F}_g^{-T} \odot \mathbf{F}_g^{-T} : \mathbf{C}$, where $(\mathbf{A} \odot \mathbf{B})_{ijkl} = A_{ik} B_{jl}$, with $\mathbf{A}$, $\mathbf{B}$ second order tensors.

A Helmholtz free-energy function $W = J W_0$, of strain energy per unit reference (grown) volume, with an explicit dependence on the elastic right Cauchy–Green strain, where W_0 is the strain-energy per unit undeformed volume, allows to satisfy the requirement of material frame indifference [8]. Recalling the dissipation inequality in material description and imposing zero dissipation under mechanical homeostasis, yields the second Piola-Kirchhoff stress:

$$\mathbf{S}^x = 2J \frac{\partial W_0}{\partial \mathbf{C}_e} : \frac{\partial \mathbf{C}_e}{\partial \mathbf{C}} = J \, \mathbf{S}_e : \mathbf{F}_g^{-T} \odot \mathbf{F}_g^{-T}, \tag{2}$$

where $\mathbf{S}_e = 2 \left(\partial W_0 / \partial \mathbf{C}_e \right)$ is an elastic second Piola-Kirchhoff stress. The superscript "x" in Equation (2) denotes *extra* stresses, representing a state out of mechanobiological equilibrium, i.e. a value of the stimulus function, $\Upsilon \neq 1$. In that sense, under mechanobiological equilibrium, if $\mathbf{F}_h = \mathbf{F}_{eh} \, \mathbf{F}_{gh}$ describes the deformation between $\mathcal{B}_0$ and any homeostatic configuration $\mathcal{B}_h$, the equilibrated Cauchy stress is defined as:

$$\boldsymbol{\sigma}_h = \boldsymbol{\sigma}_h^x - p_h \mathbf{1} = J_h^{-1} \, \mathbf{F}_h \left(\mathbf{S}_h^x + \mathbf{S}_h^p \right) \mathbf{F}_h^T = J_h^{-1} \, \mathbf{F}_h \left(\mathbf{S}_h^x - J_h \, p_h \, \mathbf{C}_h^{-1} \right) \mathbf{F}_h^T \tag{3}$$

where p_h is a Lagrange multiplier used to enforce the constraint $\Upsilon_h = 1$. Equation (3) also approximates the stress of quasi-equilibrated G&R processes, in which the characteristic rate for adaptation is faster than the rate of change of the stimulation [5,6].

Since mechanobiological equilibrium is expressed as a single nonlinear algebraic equation ($\Upsilon_h = 1$), and due to Equation (3), the stress invariants σ^i ($i = I, ..., N$), can be expressed in terms of scalar products involving $\mathbf{C}_h$, $\mathbf{S}_h^x$, J_h and p_h, allowing to determine a (generally implicit) relation that yields the (a priori unknown) volumetric contribution to stress [6].

A linearized form for the stimulus function (that neglects differences in wall shear stresses), proposed and adopted by previous works to characterize arterial tissue [5,9, 10] is, $\Upsilon(t) = 1 + K_\sigma \, \Delta\sigma(t)$, where $\Delta\sigma(t) = (\sigma^I(t)/\sigma_o^I - 1)$, K_σ is a gain parameter for mass production, $\sigma^I = \text{tr}(\boldsymbol{\sigma})$ is the first invariant of stress, and the subscript "o" denotes a quantity of an original homeostatic configuration.

The material tangent stiffness tensor involved in an incremental mechanobiologically equilibrated evolution, can be derived from the consistent linearization of Equation (2) – as a function of independent variables, J_h and $\mathbf{C}_{eh} = \mathbf{F}_{eh}^T \mathbf{F}_{eh}$ – and the consideration of an evolving homeostatic Lagrange multiplier, p_h. The Lagrange multiplier contribution is derived from the evolution – consistent with $\Upsilon_h = 1$ and $\dot{\Upsilon}_h = 0$ – of the stress term, $\mathbf{S}_h^p = -J_h p_h \, \mathbf{C}_h^{-1}$ [6]. The resulting tangent stiffness tensor lacks major symmetries in general.

3 Results

In this section, the kinematic growth model presented in Section 2, is solved for a single-layered prototypical mechanoadaptive artery. The main goal of this example is to replicate case studies from [11], which adopted a mechanobiologically-equilibrated constrained mixtures (MBE-CM) G&R model to study the initiation and progression of thoracic aortic aneurysms, assessing the influence of several risk factors.

The arterial-wall soft-tissue is modeled considering three load-bearing constituents: elastic fibers (consisting of elastin and associated microfibrils, denoted by a superscript "e"), collagen fibers (denoted by a superscript "c") and smooth muscle cells (denoted by a superscript "m"); with mass fractions – ratios between equilibrated, constituent-specific current mass densities and the current overall mass density of the tissue, the latter assumed constant – ϕ^e, ϕ^c and ϕ^m respectively, satisfying $\phi^e + \phi^c + \phi^m = 1$. The original mass fractions, ϕ_o^e, ϕ_o^c and ϕ_o^m, are related to their evolved counterparts by the Piola transformation, $\phi_h^\xi = \phi_o^\xi / J_h$ ($\xi = e, c, m$) [6].

Since the kinematic growth model assumes material homogeneity, we consider that all constituents turnover mass continuously (an unrealistic assumption for elastin, which is produced during the perinatal period and has a half-life of decades [6]). Letting all constituents respond to changes in stimuli with identical out-of-equilibrium stimulus functions and mass-specific rates for removal, and integrating the mass-balance equation, gives $J_h \phi_h^{\xi_i} / \phi_o^{\xi_i} = J_h \phi_h^{\xi_j} / \phi_o^{\xi_j}$, ($\xi_i, \xi_j = e, c, m$). Therefore, under these assumptions, current mass fractions are constant with time, i.e. $\phi_h^\xi = \phi_o^\xi = \phi^\xi$.

For the hyperelastic response, we take into account the contribution of three constituents via a standard rule-of-mixtures, $W_0 = \phi^e W_0^e + \phi^c W_0^c + \phi^m W_0^m$. The amorphous elastin-dominated matrix is modeled using a Neo-Hooke model, $W_0^e = (c^e/2) \, (\mathbf{F}_e \mathbf{G}^e : \mathbf{F}_e \mathbf{G}^e - 3)$, where c^e is a shear modulus and $\mathbf{G}^e = G_r^e \, \mathbf{a}_r \otimes \mathbf{a}_r + G_\theta^e \, \mathbf{a}_\theta \otimes \mathbf{a}_\theta + G_z^e \, \mathbf{a}_z \otimes \mathbf{a}_z$, is a (volume-preserving and symmetric) deposition stretch tensor for elastin, with $G_r^e = 1/(G_\theta^e G_z^e)$, G_θ^e and G_z^e deposition stretches for elastin along the radial (r), circumferential (θ) and axial (z) directions in the undeformed configuration – $\mathbf{a}_r$, $\mathbf{a}_\theta$ and $\mathbf{a}_z$ respectively. For the hyperelastic contribution of collagen and smooth muscle cells, we assume Fung-type models:

$$ W_0^\alpha = \frac{c_1^\alpha}{4c_2^\alpha} \sum_{i=1}^n \exp\left[c_2^\alpha \left(\mathbf{C}_e \, G^{\alpha 2} : \mathbf{a}_i^\alpha \otimes \mathbf{a}_i^\alpha - 1 \right)^2 \right] - 1, \quad (\alpha = c, m), \qquad (4) $$

where c_1^α, c_2^α are material parameters, $\mathbf{a}_i^\alpha$ are unit vectors along (either collagen-fibers or smooth muscle cells) orientations in the undeformed configuration and G^α are deposition stretches ($\alpha = c, m$). It is assumed that smooth muscle cells are oriented along the circumferential direction only (therefore $n = 1$ and $\mathbf{a}^c = \mathbf{a}_\theta$), whereas collagen-fibers are considered oriented along the axial direction, circumferential direction and diagonally (at angles $\pm\alpha_0$ with respect to the axial direction), therefore $n = 4$, further incorporating orientation-specific fractions, β_z, β_θ and $\beta_d = 1 - \beta_z - \beta_\theta$, for the

axial, circumferential and diagonal directions respectively [12]. Following [13], the referential angle α_{0h} of diagonal collagen fibers families is set to evolve during G&R according to, $\tan \alpha_{0h} = (\lambda_\theta/\lambda_z) \tan \alpha_0$, where λ_θ and λ_z are local circumferential and axial stretches (see [6]).

Deposition stretch tensors are time (and/or space) dependent entities specific to the constrained mixtures G&R model that represent newly deposited constituents [5, 6]. In these examples, deposition stretches are considered constant and are included in order to attain the same order of magnitude for strain-energy to that reported by [11].

The set of (baseline) material parameters for an illustrative mouse descending thoracic aorta, adopted from [11] and used in the examples of this work, are listed in Table 1.

Constituent mass fractions	ϕ^e, ϕ^m, ϕ^c	0.34, 0.33, 0.33
Collagen relative fractions	β_z, β_θ, β_d	0.056, 0.067, 0.877
Elastic material parameters	c^e, c_1^m, c_2^m	89.71 kPa, 261.4 kPa, 0.24
	c_1^c, c_2^c	234.9 kPa, 4.08
Diagonal collagen orientation	α_0	29.9 deg
Deposition stretches	G_θ^e, G_z^e G^m, G^c	1.90, 1.62, 1.20, 1.25

Table 1: Representative baseline model parameters for a mouse descending thoracic aorta (adopted from [11]) used in the examples performed in this work.

We implemented the present rate-independent kinematic-growth framework for G&R in the open source software FEBio [14]. From a numerical perspective, the implementation resembles that of a hyperelastic material with a non supersymmetric tangent stiffness tensor.

Solutions proceed in two stages. In Stage I, the (pre-stressed) original-homeostatic in-vivo state is computed. At the end of Stage I, the volumetric Cauchy stress (σ_{vo}) is stored, which plays the role of a (local) material parameter for Stage II. In Stage II, the particular equilibrated solution for this G&R formulation (the evolved-homeostatic configuration) is determined. To that end, we assume an isotropic volumetric growth deformation gradient, following earlier studies that have adopted it for modeling of stress-driven cardiac [15] and arterial-wall growth [16].

We consider a 3D finite element (FE) geometry (shown partially in Figure 1) of an initially cylindrical arterial segment with inner radius a_0, thickness h_0, and length $l_0 = 15$ mm in its undeformed configuration. The FE mesh comprises $N_r N_\theta N_z = 1 \times 20 \times 20 = 400$ displacement-based 3D quadratic elements with full 3×3×3 Gauss integration, which showed consistent results when compared to other discretizations in a mesh convergence study [11]. We fixed axial displacements at both ends, with rigid body motions suppressed. As an external (pre-)load, we apply an in-vivo value of blood pressure ($P_o = 13.98$ kPa) on the inner surface of the cylinder and compute

the inner radius $a_o = 0.647$ mm, thickness $h_o = 0.04$ mm, and length $l_o = l_0$, of the original homeostatic configuration.

Quasi-static analyses were performed in 10 incremental steps, without line searches during Newton-Raphson iterations. Elapsed total CPU times ~ 1 min on a single CPU processor at 2GHz in a Lenovo ThinkBook-14-G2 with 16GB RAM.

To drive quasi-static G&R FE simulations, following [6, 11] we consider an degradation of elastin and loss of collagen cross-linking, while preserving inner pressure ($P_h = P_o$). Elastin degradation and loss of collagen cross-linking are achieved by reductions of the material parameters c^e and c_1^c respectively, localized at an axial coordinate $z_{om} = l_o/2$ and a circumferential coordinate $\theta_{om} = \pi$ (both in the reference homeostatic configuration) and are set to diminish gradually with distance to an axial coordinate z_o and a circumferential coordinate θ_o. If ϕ is a property to be locally reduced, then:

$$\phi(z_o, \theta_o) = \phi_{\text{end}} + (\phi_{\text{cen}} - \phi_{\text{end}}) \exp \left(- \left| \frac{z_o - z_{om}}{s_o} \right|^\nu \right) \exp \left(-f \left| \frac{\theta_o - \theta_{om}}{s_\theta} \right|^\nu \right), \ (5)$$

where $z_o \in [0, l_o]$ and $\theta_o \in [0, 2\pi]$, $\nu = 5$ is an exponential decay parameter and $s_z = 2.5$mm, $s_\theta = \pi/3$ are deviation parameters for the axial and circumferential direction respectively. Moreover, ϕ_{end} and ϕ_{cen} are values of the parameter near the ends ($z_o = 0, l_o$) or within the central/apex ($z_o = l_o/2, \theta_o = \pi$) regions of the computational aorta. For axisymmetric lesions $f = 0$, and for asymmetric lesions, $f = 1$.

We performed simulations using both the current mechanobiologically equilibrated kinematic growth (MBE-KG) model and the mechanobiologically equilibrated constrained mixtures (MBE-CM) model [3, 5, 6, 11], in order to examine the differences in the response between methods.

We simulated different conditions (severity of lesions) depending on the method used (either MBE-CM or MBE-KG), and type of aneurysm (either axisymmetric or asymmetric), aiming at capturing the same maximum dilatation with both methods. For axisymmetric lesions, we applied a 51% loss of elastic fiber integrity in the CM model and a 100% degradation of elastin along with a 80% loss of collagen cross-linking in the KG model, to reach a maximum dilatation of 220% with both methods (Figure 1, A and B). To induce asymmetrical lesions, we applied a 44% reduction of elastic fiber integrity using the CM model. In the KG model, we again introduced complete elastin degradation and a 99% decline in collagen cross-linking; leading to a maximum dilatation of 58% using both approaches (Figure 1, C and D). Therefore, in both types of aneurysms, the KG method required a higher severity of injury compared to the CM method in order to achieve a similar response.

Figure 1 reveals that the mechanical response is not isochoric. Particularly, as stated by [11], graded localized losses of elastic fiber integrity and collagen-fiber cross-linking can result in G&R responses that cause localized volume change (dilatation) of the aortic wall.
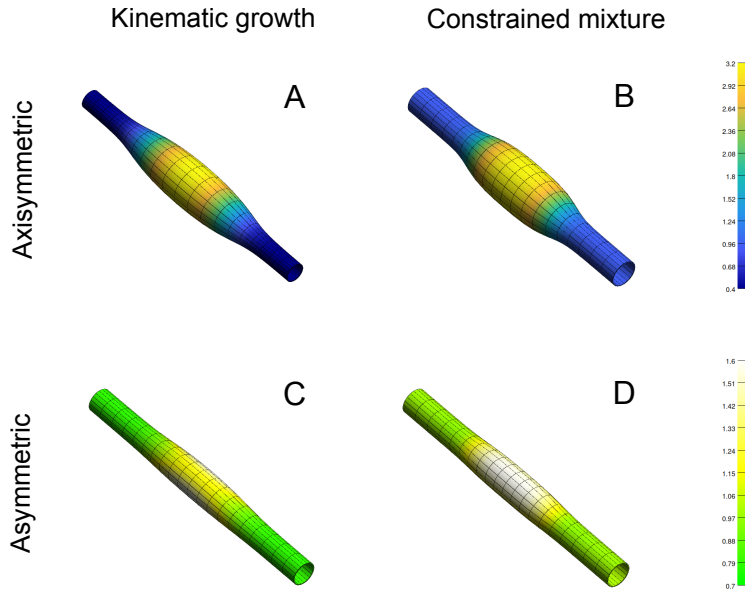
Figure 1: Relative volume of fully developed, mechanobiologically equilibrated, axisymmetric (A, B) and asymmetric (C,D) dilatations of an initially cylindrical aortic segment caused by a localized loss of elastic fiber integrity and collagen-fiber cross-linking – reduction of parameters c^e and c_1^c according to Equation (5) – using the mechanobiologically-equilibrated (MBE) kinematic growth model (first column) and the MBE constrained-mixtures model (second column).

Moreover, decrements in volume are observed in all cases at the end regions of the computational model, indicative of a mechanical maladaptation due to elastin degradation and loss of collagen cross-linking (Figure 1).

Disagreements between the response of the current MBE-KG model and the MBE-CM model, can be explained by differences in the formulation of the methods. Specifically, in the CM model mass fractions per unit current volume are variable with time, whereas under the assumption of material homogeneity, mass fractions in the KG model remain constant. Moreover, in the CM model formulated and adopted by [5, 6, 11], turnover of elastin is not allowed since G&R times considered therein are shorter than the half-life of that constituent. These fundamental methodological and physiological discrepancies between MBE formulations affect both stress and stiffness.

The ability of the current MBE-KG model at replicating the response of the MBE-CM model could be improved by adopting a different, more complex or appropriate form for the growth deformation tensor $\mathbf{F}_g$. For instance, the isotropic volumetric form utilized here can be replaced by an anisotropic (transversely isotropic) growth deformation tensor, arguably more suitable to account for the characteristic arterial wall microstructure by incorporating preferential growth directions [15, 17, 18].

4   Conclusions

In this work, we propose a mechanobiologically equilibrated, steady-state formulation for the finite kinematic G&R theory of soft tissues.

The formulation is time-independent, therefore, for a given set of external stimuli, integration over the time domain and tracking the production and removal history is unnecessary, saving computation time.

For illustrative purposes, the method is applied to examples of axisymmetric and asymmetric aneurysms on a single-layered, idealized cylindrical artery.

The current mechanobiologically-equilibrated kinematic growth theory is able to achieve grown and remodeled, steady-state configurations of soft tissues with intricate geometries and/or loads within a finite-element framework, and its capabilities mainly rely on being able to predict long-term outcomes, which arguably matters most to medical professionals and patients [5, 19].

Despite its advantages, the current time-independent formulation is generally ineffective for the analysis of truly time-dependent responses of soft tissues, where the full time-dependent formulation will continue to be required in order to determine the evolution of the growth process under particular physiological and pathophysiological scenarios.

Further research is required to improve the understanding about the characteristics of mechanical stimuli driving the G&R process.

References

[1] W.B. Cannon, "Organization for physiological homeostasis", Physiological reviews, 9(3), 399-431, 1929. DOI: 10.1152/physrev.1929.9.3.399.

[2] C.J. Cyron, J.D. Humphrey, "Growth and remodeling of load-bearing biological soft tissues", Meccanica, 52, 645-664, 2017. DOI: 10.1007/s11012-016-0472-5.

[3] M. Latorre, "Modeling biological growth and remodeling: contrasting methods, contrasting needs", Current Opinion in Biomedical Engineering, 15, 26-31, 2020. DOI: 10.1016/j.cobme.2019.11.005.

[4] E.K. Rodriguez, A. Hoger, A.D. McCulloch, "Stress-dependent finite growth in soft elastic tissues", Journal of biomechanics, 27(4), 455-467, 1994. DOI: 10.1016/0021-9290(94)90021-3.

[5] M. Latorre, J.D. Humphrey, "A mechanobiologically equilibrated constrained mixture model for growth and remodeling of soft tissues", ZAMM-Journal of Applied Mathematics and Mechanics/Zeitschrift für Angewandte Mathematik und Mechanik, 98(12), 2048-2071, 2018. DOI: 10.1002/zamm.201700302.

[6] M. Latorre, J.D. Humphrey, "Fast, rate-independent, finite element implementation of a 3D constrained mixture model of soft tissue growth and remodeling", Computer methods in applied mechanics and engineering, 368, 113156, 2020. DOI: 10.1016/j.cma.2020.113156.

[7] J.D. Humphrey, K. Rajagopal, "A constrained mixture model for growth and remodeling of soft tissues", Mathematical models and methods in applied sciences, 12(3), 407-430, 2002. DOI: 10.1142/S0218202502001714.

[8] D. Ambrosi, M. Ben Amar, C.J. Cyron, A. DeSimone, A. Goriely, J.D. Humphrey et al., "Growth and remodelling of living tissues: perspectives, challenges and opportunities", Journal of the Royal Society Interface, 16(157), 20190233, 2019. DOI: 10.1098/rsif.2019.0233.

[9] M. Latorre, J.D. Humphrey, "Critical roles of time-scales in soft tissue growth and remodeling", APL bioengineering, 2, 026108, 2018. DOI: 10.1063/1.5017842.

[10] M. Latorre, J.D. Humphrey, "Mechanobiological stability of biological soft tissues", Journal of the Mechanics and Physics of Solids, 125, 298-325, 2019. DOI: 10.1016/j.jmps.2018.12.013.

[11] M. Latorre, J.D. Humphrey, "Numerical knockouts–In silico assessment of factors predisposing to thoracic aortic aneurysms", PLoS computational biology, 16(10), e1008273, 2020. DOI: 10.1371/journal.pcbi.1008273.

[12] M. Latorre, J.D. Humphrey, "Modeling mechano-driven and immuno-mediated aortic maladaptation in hypertension", Biomechanics and modeling in mechanobiology, 17, 1497-1511, 2018. DOI: 10.1007/s10237-018-1041-8.

[13] J. Wilson, S. Baek, J. Humphrey, "Importance of initial aortic properties on the evolving regional anisotropy, stiffness and wall thickness of human abdominal aortic aneurysms", Journal of The Royal Society Interface, 9(74), 2047-2058, 2012. DOI: 10.1098/rsif.2012.0097.

[14] S.A. Maas, B.J. Ellis, G.A. Ateshian, J.A. Weiss, "FEBio: Finite Elements for Biomechanics", Journal of Biomechanical Engineering, 134(1), 011005, 2012. DOI: 10.1115/1.4005694.

[15] S. Göktepe, O.J. Abilez, E. Kuhl, "A generic approach towards finite growth with examples of athlete's heart, cardiac dilation, and cardiac wall thickening", Journal of the Mechanics and Physics of Solids, 58(10), 1661-1680, 2010. DOI: 10.1016/j.jmps.2010.07.003.

[16] E. Kuhl, R. Maas, G. Himpel, A. Menzel, "Computational modeling of arterial wall growth: Attempts towards patient-specific simulations based on computer tomography", Biomechanics and modeling in mechanobiology, 6, 321-331, 2007. DOI: 10.1007/s10237-006-0062-x.

[17] P. Sáez, E. Peña, M.A. Martínez, E. Kuhl, "Computational modeling of hypertensive growth in the human carotid artery", Computational mechanics, 53, 1183-

1196, 2014. DOI: 10.1007/s00466-013-0959-z.

[18] J. Vastmans, L. Maes, M. Peirlinck, E. Vanderveken, F. Rega, E. Kuhl, et al., "Growth and remodeling in the pulmonary autograft: Computational evaluation using kinematic growth models and constrained mixture theory", International Journal for Numerical Methods in Biomedical Engineering, 38(1), e3545, 2022. DOI: 10.1002/cnm.3545.

[19] J.W. Holmes, J.E. Wagenseil, "Spotlight on the future of cardiovascular engineering: Frontiers and challenges in cardiovascular biomechanics", Journal of biomechanical engineering, 138(11), 110301, 2016. DOI: 10.1115/1.4034873.